Saint Petersburg
RUSSIA

B23

History Match and Polymer Injection Optimization in a Mature Field Using the Ensemble Kalman Filter

S. Raniolo* (eni e&p), L. Dovera (eni e&p), A. Cominelli (eni e&p), C. Callegaro (eni e&p) & F. Masserano (eni e &p)

SUMMARY

The paper focuses on a Chemical EOR study for a mature field. The field was selected due to its volume in place and good petrophysical properties. Indeed, the preliminary screening gave indication that polymer injection could be a promising EOR technique. New core data, SCAL and PLT were acquired and a high resolution model of the pilot area was built to integrate such new data and to properly capture the behaviour of the chemicals.
The sector modelling was challenging due to the complexity of the history match and polymer injection optimization. The field has been producing for 60 years. Moreover, due to the complex structural settings, the sector model is not completely isolated from the full field model and dummy wells were introduced to mimic the flow interaction with the rest of the reservoir.
A Computer Assisted History Matching (CAHM) was carried out by the means of the Ensemble Kalman Filter (EnKF). The EnKF is a Monte-Carlo method that automatically updates an ensemble of reservoir models by production data integration. The EnKF is capable of providing a set of matched models that preserve the geological coherence which can be used to quantify uncertainty in forecast production.
In this paper, we present the application of the EnKF to history match the sector model and the consequent optimization for polymer injection. EnKF was used to calibrate petrophysical properties, relative permeability and faults transmissibility integrating measurements, shut-in pressures and rates, of 14 wells including the dummy wells. The final output is a set of 100 alternative models that properly match production data which were used to set up and optimize the forecast development strategy through polymer injection.
This application provides evidence that the EnKF is effective and efficient for history matching. Moreover, dealing with multiple models put the basis for a conscious estimation of future production and a more realiable risk evaluation on EOR strategy.

Introduction

This work documents the reservoir modelling study developed as part of the company's effort to implement a pilot chemical Enhanced Oil Recovery (EOR) project in a giant on-shore brown field. The aim of the study was to quantify the benefit of the EOR project in terms of expected cumulative oil production and associated net present value (NPV), providing also confidence intervals which accounted for the geological/engineering uncertainty and availability of production data. To achieve these results, it was essential to implement a workflow where ensemble based methods such as the Ensemble Kalman Filter (EnKF) and the Ensemble Optimisation (EnOpt) are essential and distinctive components, [13], [6].

The field at hand is composed by 12 heavily faulted reservoirs included in four main Zones. The deposits are turbiditic and deltaic sandstone with interbedded shales and anhydrite intercalations ranging from Lower to Upper Miocene Age. From a structural point of view, the field could be described as a NNW-SSE direction anticline cut by 2 major faulting systems. The production started up as primary depletion in 1953, then water injection was gradually implemented in the different reservoirs and nowadays the field is under secondary recovery by means of peripheral water flooding, with high water-cut in most of the wells.

According to the reservoir rock and fluid properties, a preliminary screening gave indication that polymer injection could be a promising chemical EOR technique for the field. Indeed, the water flooding is characterised by an unfavourable mobility ratio, hence the volumetric efficiency of the process may be improved by means of a more favourable mobility ratio as a results of a polymer solubilised in the injected water. The next step was the selection of a suitable area for polymer injection. The area was chosen according to various criteria, including the presence of remarkable oil in place, a low actual recovery factor, good petrophysical properties, and the possibility to implement a careful reservoir monitoring process to evaluate the benefits.

The pilot area is shown in *Figure 1*. To better characterize the reservoir, the entire thickness of the pilot area was cored taking the opportunity of a vertical well targeting deeper objectives in the field. Then, a comprehensive experimental program was executed, including routine and special core analysis. This provided detailed information on the petrophysical properties of the area, including an improved porosity/permeability correlation.
In addition, an oil sample was acquired at the wellhead of the dedicated producer P6. This dead oil sample allowed a tuning of the polymer rheological properties at reservoir temperature and water formation salinity using commercial compositions. Moreover, the polymer adsorption and the residual resistance factor were measured trough a core flooding in the laboratories [3].

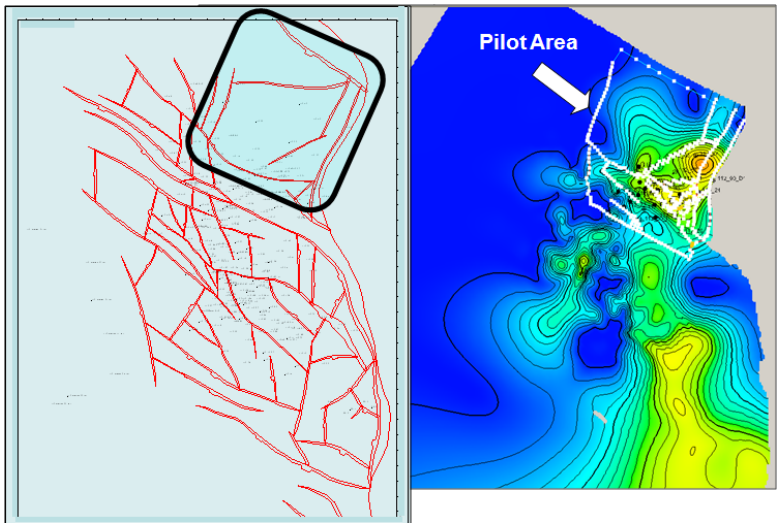

Figure 1 *Pilot area for the EOR application.*

The evaluation of a chemical EOR project by means of reservoir modelling requires attention on reservoir heterogeneity and uncertainty. Indeed, heterogeneity drives water in the reservoirs while uncertainty in the reconstruction of the subsurface impacts the confidence of the expect recovery due to EOR.
The actual full field model poorly characterized the pilot area, which was only represented by a single thick layer with cell spacing of 200 x 200 m^2. This resolution is not enough for a chemical EOR study, which typically requires much more details both vertically and laterally. Therefore, a sector model was needed in order to better capture properties and heterogeneities of the pilot area.
To manage the uncertainty in a robust manner, the whole reservoir modelling workflow, from geological model construction and history matching to forecast, was developed using statistical ensemble based methodologies. In this framework, multiple static and dynamic models were realized integrating all the new data. Secondly, a multiple history matching was achieved using the EnKF approach. Finally, a polymer optimization on the multiple history matched models was performed to define the development strategy. This process, where production data are first assimilated and then engineering controllable parameters are optimised, may be seen as the first iteration of Closed Loop Reservoir Management as presented in various papers these years, [16]. Then this work will also be used as building block for the reservoir management of the field, with integration of process monitoring and optimisation.

Geological and dynamical description of the sector model

The sector model was based on a fine grid and a detailed vertical layering. New property distributions and new relative permeability curves were adopted integrating the latest laboratory measurements. CPI data were used to define NTG, porosity and irreducible water saturation modelling. The pay intervals were identified in the wells log using a porosity cut-off of 8% (from the full-field model). The resulting sand-flag was scaled-up in the 3D grid taking into account possible shoulder effects and small mismatches between well tops and logs. A variographical analysis carried out for each zone, showed that the database was suited to use the Sequential Gaussian simulation algorithm (SGSim, [11]) to propagate the NTG values all over the reservoir using seismic/sedimentological derived trend maps. Comparison between porosity and NTG data showed a poor correlation thus porosity was distributed using SGSim with different trends maps. Clear correlation existed between porosity and irreducible water saturation so a deterministic function was used to distribute saturation values.
Taking into account also data from the new cored well, a new relationship between horizontal log-permeability (Ln-K) and porosity was determined. Using this relationship, Ln-K trend maps were computed from the porosity trends, then Ln-K was distributed using collocated Co-Kriging simulation with a correlation coefficient of 0.8. A deterministic function was used to compute vertical permeability from horizontal permeability.

The main characteristics of the sector model are the following:

- Areal dimensions: 5 km long x 4.5 km wide
- Average cell dimensions: 50 m x 50 m
- Active cells: 51168 cells
- Number of layers: 8

Purposely, the same simulation grid was used also for the simulation phase to avoid any error due to upscaling and to make easier a consistent update of the geological properties in the history matching phase.

Special Core Analysis (SCAL) were performed on plugs of the new core, namely: Amott wettability, water-oil relative permeability curves and capillary pressure. The results were not fully reliable, see *Figure 2*. Indeed, irreducible water saturation lower than 0.25 is associated to oil wettability, but the saturation cross point around 50% indicates mixed wettability and low water endpoint (Krwr) is typical of a water wet system, [22].

For these reasons, Krwr was considered as uncertain and tuning parameter during the history matching process.

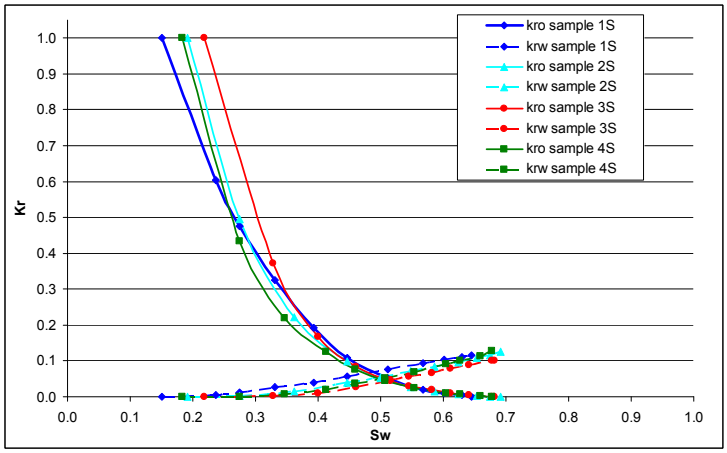

Figure 2 *Normalised water-oil relative permeability curves for different samples.*

The pilot area comprises a total of 22 drilled wells, some of which are commingled with other reservoirs in the field. The absence of PLTs and back allocated data for these commingled wells imposed to retrieve production data from the original full field model. This process involved the evaluation of the liquid fraction f_{LIQ} (i.e. ratio between the simulated liquid production of the pilot area divided by the total simulated liquid rate):

$$f_{LIQ} = \frac{Pilot\ area\ simulated\ liquid\ rate}{Total\ simulated\ liquid\ rate}$$

This quantity allowed to rescale the historical production data of a well with respect to the portion due to the pilot area contribution. As a consequence, high uncertainty was associated to such data during the history match process.
The geology of the pilot area is characterized by a major fault system in the NNW-SSE direction with high displacements as showed in *Figure 3*. Along that system, different reservoirs may communicate due to the high fault throws.

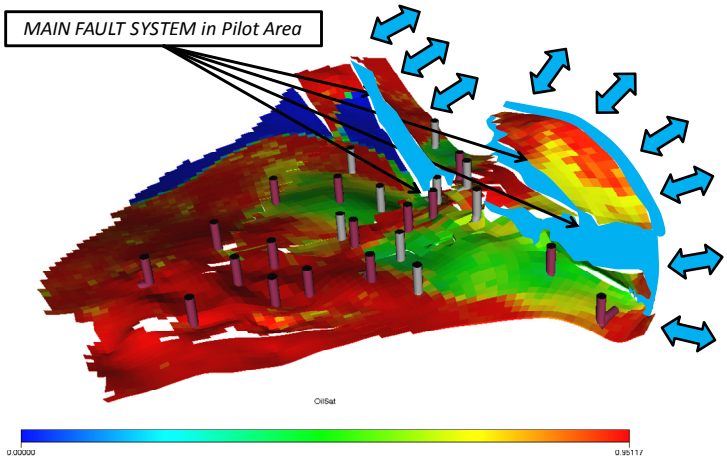

Figure 3 *Main faults system for the pilot area: the arrows highlight the connections between the pilot area and the rest of the reservoir.*

In particular, the pilot area communicates with reservoirs in Zone II, Zone III and Zone IV. Indeed, pressures of dedicated wells P2 and P7 are supported by the water injection in Zone II and Zone IV, as highlighted in *Figure 4*.

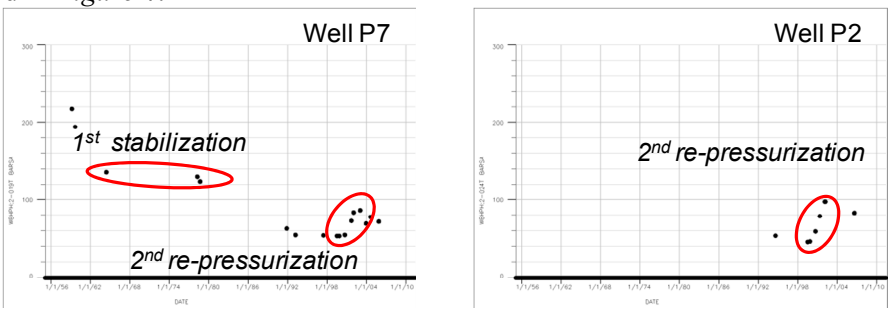

Figure 4 *Historical pressure data for two producers perforated only in the pilot area.*

In order to mimic the flow interaction between the pilot area and the rest of the field, dummy wells were introduced.

- *4 dummy water injectors* were used to simulate the historical flow interaction with Zone III and Zone IV before water injection start up in April 2003. The pilot area historically recorded lower pressure respect to other reservoirs. Therefore, dummy water injectors were introduced to mimic the water flux coming into the area, see *Figure 5*. These wells were simulated under water rate controls.

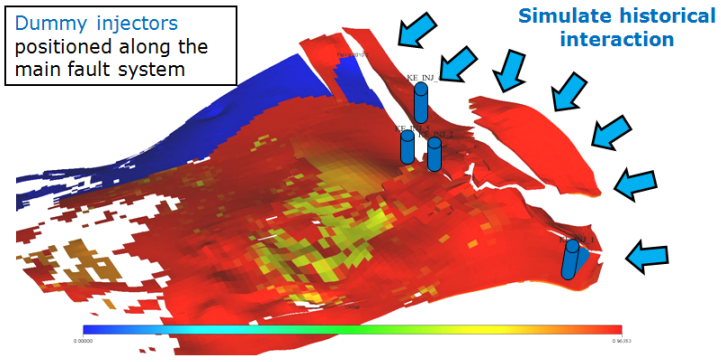

Figure 5 *Dummy water injectors in the sector model.*

- *3 dummy water producers* were add to correctly manage the re-pressurization of the pilot area after the water injection start up in April 2003 when the average pressure of the pilot area started to be higher with respect to other reservoirs. These wells were simulated under bottom-hole pressure controls, *Figure 6*.

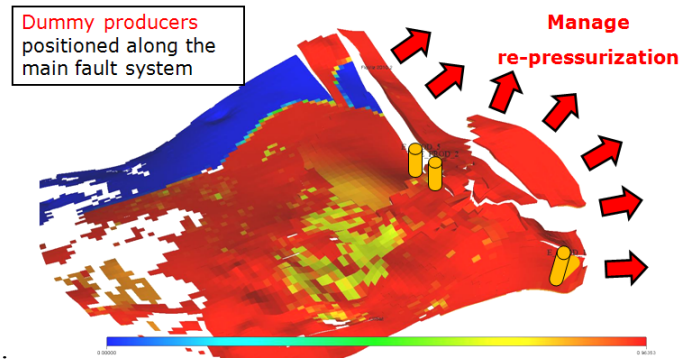

Figure 6 *Dummy water producers in the sector model.*

Introduction to the Ensemble Kalman Filter (EnKF)

The Ensemble Kalman Filter (EnKF) is a Monte Carlo data assimilation technique for high dimensional problems. In the last years, the method has become a popular approach in reservoir simulation community for history matching and application on real cases have been published, [1], [3], [9], [19].
There are three basic steps in the EnKF algorithm.

1. *Generation of the initial ensemble*: an ensemble of reservoir models is generated according to the prior uncertainty varying geological and/or dynamic parameters with geostatistics and/or Monte Carlo sampling.
2. *Forecast step*: the models of the ensemble are simulated in time using the flow simulator (Eclipse).
3. *Assimilation (or Update) step*: when measurements are available, the models are updated to integrate data using an error minimizing scheme. The assimilation step is a correction step to honour the observations.

The initial ensemble is created only at the beginning, forward and assimilation steps are continuously alternated until the end of the flow simulation.
In general, in the EnKF the state variable $\mathbf{y}$, describing the reservoir model includes 3 types of parameters: static parameters $\mathbf{m}_s$ (e.g. porosity or permeability), dynamic parameters $\mathbf{m}_d$ (e.g. pressures and saturations) and production data $\mathbf{d}$ (e.g. wells rates, wells pressures) i.e.

$$\mathbf{y} = \begin{bmatrix} \mathbf{m}_s \\ \mathbf{m}_d \\ \mathbf{d} \end{bmatrix}$$

The ensemble of models is then represented by an ensemble of state vectors $\{\mathbf{y}_{k,j}\}_{j=1}^{N_e}$ where j is the index that identifies the model in the ensemble, k is the time step index of the flow simulation. The ensemble of state vectors is continuously updated at each flow simulation step where measurements are available. In particular, during the forward step, the flow simulation is run on each reservoir model (i.e. state vector):

$$\mathbf{y}_{k,j}^{f} = F(\mathbf{y}_{k-1,j}^{u}), \quad j = 1,\ldots,N_e$$

where F is the forward model and superscript f denotes the forecast, meaning that the values are output from the simulator before Kalman filter updating. In this step, only the dynamic variables are modified since the models evolve in time. Then the assimilation step is performed: here the state vectors are updated using the following update equation:

$$\mathbf{y}_{k,j}^{u} = \mathbf{y}_{k,j}^{f} + \mathbf{K}_k(\mathbf{d}_{k,j}^{obs} - \mathbf{H}_k\mathbf{y}_{k,j}^{f}).$$

The matrix $\mathbf{H}_k$ selects the simulated data from the state vector. The matrix $\mathbf{K}_k$ is called Kalman gain matrix and is given by

$$\mathbf{K}_k = \mathbf{C}_{\mathbf{y},k}^{f}\mathbf{H}_k^{T}(\mathbf{H}_k\mathbf{C}_{\mathbf{y},k}^{f}\mathbf{H}_k^{T} + \mathbf{C}_{\mathbf{d}})^{-1}$$

where $\mathbf{C}_{\mathbf{y},k}^{f}$ is the covariance matrix for the state variables computed directly from the ensemble of forecasted results $\left\{\mathbf{y}_{k,j}^{f}\right\}_{j=1}^{N_e}$ with the standard statistical formula i.e.

$$\mathbf{C}_{\mathbf{y},k}^{f}=\frac{1}{N_e-1}\sum_{j=1}^{N_e}(\mathbf{y}_{k,j}^{f}-\bar{\mathbf{y}}_k)(\mathbf{y}_{k,j}^{f}-\bar{\mathbf{y}}_k)^T \text{ and } \bar{\mathbf{y}}_k=\frac{1}{N_e}\sum_{j=1}^{N_e}\mathbf{y}_{k,j}^{f}.$$

The vector $\mathbf{d}_{k,j}^{obs}$ is a vector that contains observed production data perturbed with random measurement error $\boldsymbol{\varepsilon}_j$ sampled from a normal distribution $N(\mathbf{0},\mathbf{C}_\mathbf{d})$ with a diagonal positive definite matrix $\mathbf{C}_\mathbf{d}$: $\mathbf{d}_{k,j}^{obs}=\mathbf{d}_{k}^{obs}+\boldsymbol{\varepsilon}_j$. With the update equation, both static variables and dynamic variables are modified based on the Kalman Gain multiplied by the data misfit (difference between observed data and simulated data).
In *Figure 7*, the typical EnKF workflow between two consecutive time steps is illustrated.
In terms of implementation, the cost of the updating is negligible compared to the cost of the flow simulation. In addition, because of the restarting capabilities of the flow simulator, after each assimilation step, the flow simulation can be restarted from the correspondent time step. Therefore, the final cost of the workflow is equivalent to the cost of one flow simulation for each realization.
However, there are some limitations in the use of the EnKF. In particular, it can be proven that the EnKF updating is exact only for linear dynamics and Gaussian assumption and with an infinite ensemble size, [5], [17]. On the basis of this, in the standard EnKF practice, the parameters of the final ensemble are rerun from the beginning of the flow simulation to guarantee the final consistency in terms of pressure and saturations.

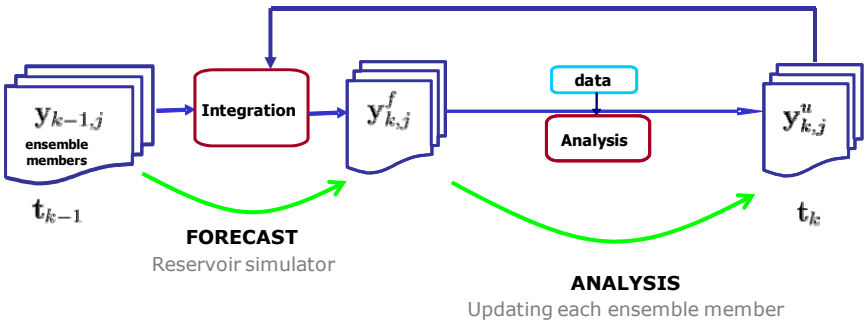

Figure 7 *EnKF workflow.*

Implementation of EnKF to history match the pilot area

In this work, the initial ensemble was generated according to the model uncertainty highlighted during the reservoir study. In particular, the following uncertainty parameters were chosen:

- Net To Gross (NTG)
- Porosity
- Permeability (Ln-K)
- Irreducible water saturation
- Relative permeability
- Fault transmissibility

NTG, porosity and permeability are spatial variables distributed in the reservoir grid with geostatistics. In order to build the ensemble, multiple geostatistical simulations were generated following the geological workflow. Therefore, the final realizations were constrained to all the data (core data, seismic/sedimentological trends, correlations, etc.).
The other uncertain parameters in the ensemble are scalar ones thus Monte-Carlo sampling was used to generate multiple values. In particular, the relative permeability end-points (Krwr) were varied sampling uniformly the values within the interval [0.3 0.5].
Uncertainty on fault transmissibility, due to structure uncertainty, was considered after a sensitivity analysis highlighted their impact on well connectivity. In particular, 5 main faults were considered as critical to achieve the history match, see Figure 8. These main faults were connected by means of Non-Neighbour Connections (NNC) and the correspondent transmissibility was considered a history matching parameter. In conclusion, the fault parameters used in the ensemble are 5 scalar values sampled within the interval [0 2] that are used as exponents to vary the transmissibility of the 5 NNC between [1 10^2].

An initial ensemble of 100 realizations of spatial and scalar parameters was generated.

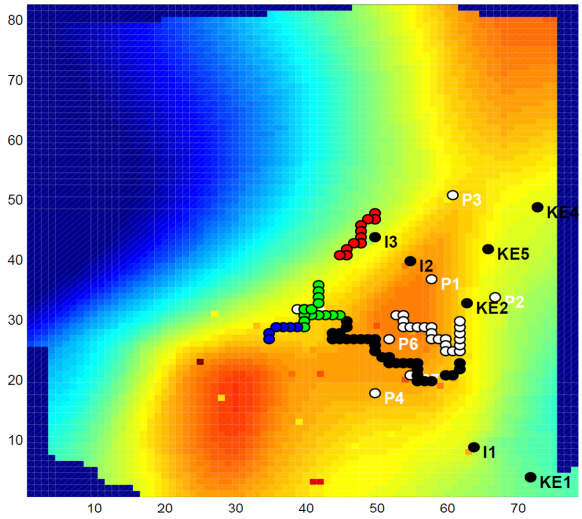

Figure 8 *Five main faults selected as history matching parameters.*

The EnKF was used to match the wells (6 producers and 2 injectors) strictly dedicated to the pilot area and the dummy injectors.
In particular, the following measurements were considered:

- Producers: shut-in pressures, oil, water and liquid rates;
- Injectors: shut-in pressures, injection rates;
- Dummy injectors: injection rates.

The production and injection controls are produced liquid rates and water injection rates. The following measurement errors were used for the EnKF assimilation steps:

- Oil rate: 0.08%
- Water rate: 0.15%
- Liquid rate: 1 stb/day
- Injection rate: 50 stb/day
- Shut-in pressure: 10 barsa

For computational efficiency, the EnKF was not activated at each time step, but data were assimilated only when shut-in pressure measurements were available: in total 42 assimilation time steps were implemented.

Localization strategy

EnKF updating is based on the Kalman gain matrix that contains correlations between simulated data and model parameters. The increasing of the ensemble size improves the estimation of the covariance and consequently the performance of the filter, [2], [15]. In large scale problems, the number of parameters is very large while the size of the ensemble is limited by computational reasons and only small ensemble can be used. In this case, correlations are well estimated only close to the conditioning data; far from observations, because of sampling error, correlations are meaningless or "spurious" in EnKF jargon. The problem of spurious correlations can severely deteriorate the quality and reliability of the results. In order to remove the effect of spurious correlations, a localization technique can be used, [2], [14], [15]. The main idea of localization is that the correlation between parameters and observations too far from each other should be equal to zero. There are different localization techniques, [14]. In our case, a localization based on a distance function ρ was used as proposed by Furrer and Bengtsson, [7], [14]. In particular, ρ is defined as:

$$\rho(s) = \frac{1}{1+(1+f(0)^2 / f(s)^2)/N_e}$$

where $f(.)$ is a covariance function, s is the separation distance for the covariance function and N_e is the ensemble size (the larger the ensemble the larger the range of the localization function). A spherical covariance function was applied to represent the cross-covariance between data and state variable. The function is a tapered function equal to one close at the observation location, it has a relatively flat plateau and it drops to zero rapidly as the distance from observation goes beyond the range. When localization function is used, during the updated step, the Kalman gain is premultiplied by the function ρ using the Schur product i.e.

$$\mathbf{y}_{k,j}^{u} = \mathbf{y}_{k,j}^{f} + \rho \circ \mathbf{K}_k (\mathbf{d}_{k,j}^{obs} - \mathbf{H}_k \mathbf{y}_{k,j}^{f}).$$

In this work, different function ranges and anisotropies were used according to the wells, the type of measurements and the time steps. For example, *Figure 9* shows the Kalman gain weights that were used to update the permeability (Ln-K) at the assimilation step 22 when shut-in pressure for injection well I2 was integrated. Indeed, the bottom-hole pressure match is mainly sensitive to the geological characteristics inside the drainage area; therefore an isotropic localization region around the well was selected. The localized Kalman gain was obtained by the product of the sensitivity region with the original Kalman gain. Another example of localization is shown in *Figure 10*. In this case, we show the Kalman gain for Ln-k at the assimilation step 27 when produced water rates for the well P5 was

assimilated. Since, according to the reservoir interpretation, the produced water derives from the near water injector I2, a sensitivity region that includes the couple producer-injector was drawn.

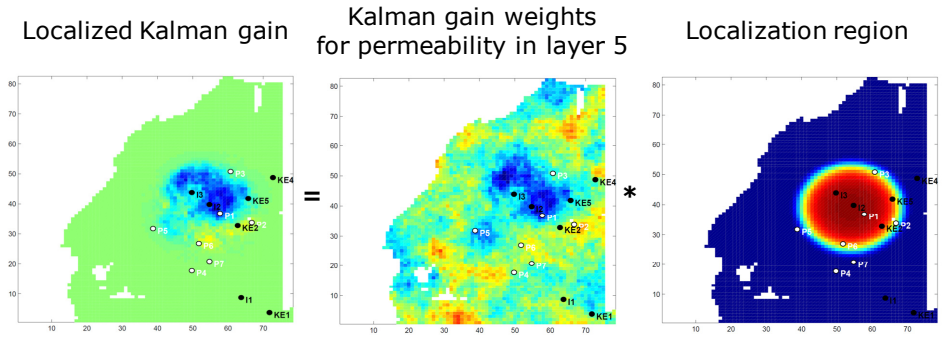

Figure 9 *Localized Kalman gain for assimilation of BHP of the water injector is the product between the Kalman gain and the localization region function.*

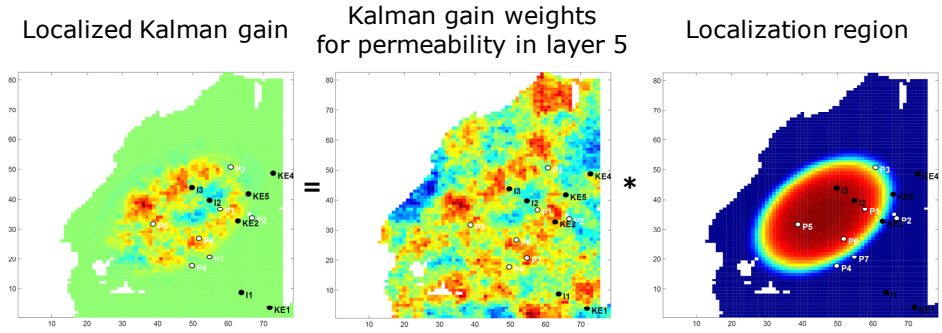

Figure 10 *Localized Kalman gain for the assimilation of produced water of the oil producer is the product between the Kalman gain and the localization region function.*

History match results

The final history match results for the key wells are reported from *Figure 11* to *Figure 13*. In these plots, the grey lines represent the simulation results of the prior ensemble (before the assimilation). The coloured lines indicate the simulation results of the posterior ensemble. Observed data are the black stars. It is interesting to note that the spread of the final realizations is reduced where measurements come available, while the initial range is well maintained where there is lack of information. In conclusion, a good quality history match was obtained.

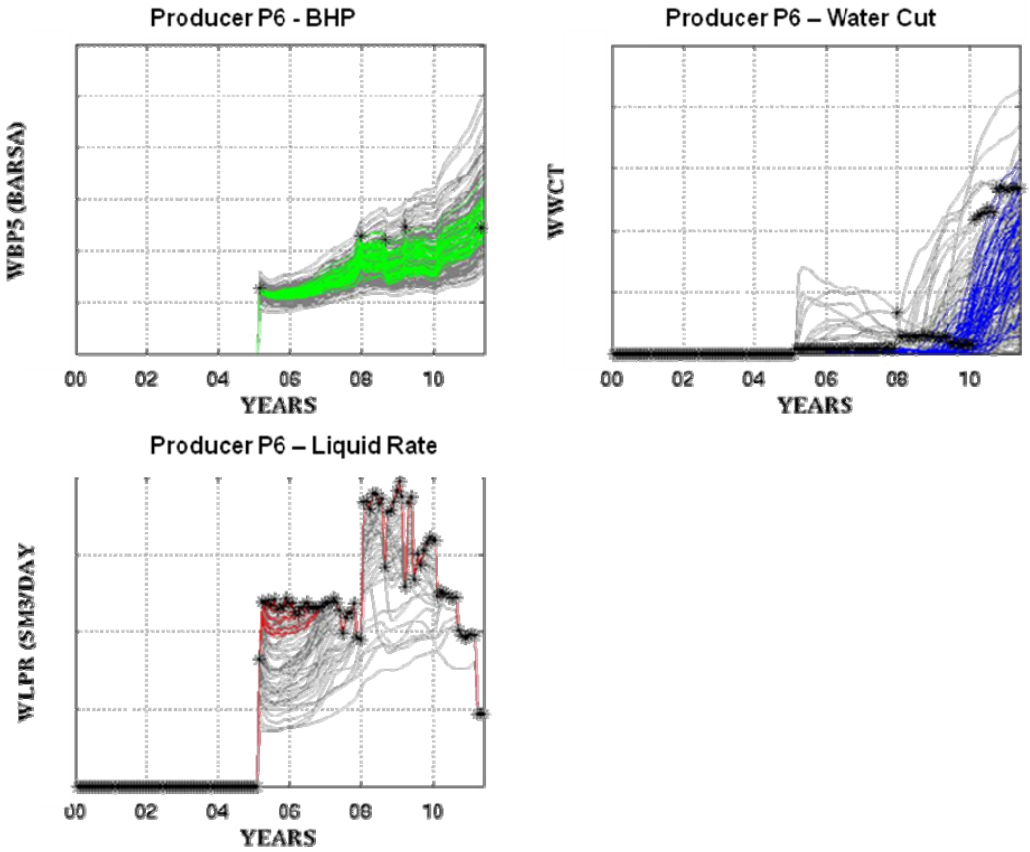

Figure 11 *History match results for Producer P6.*

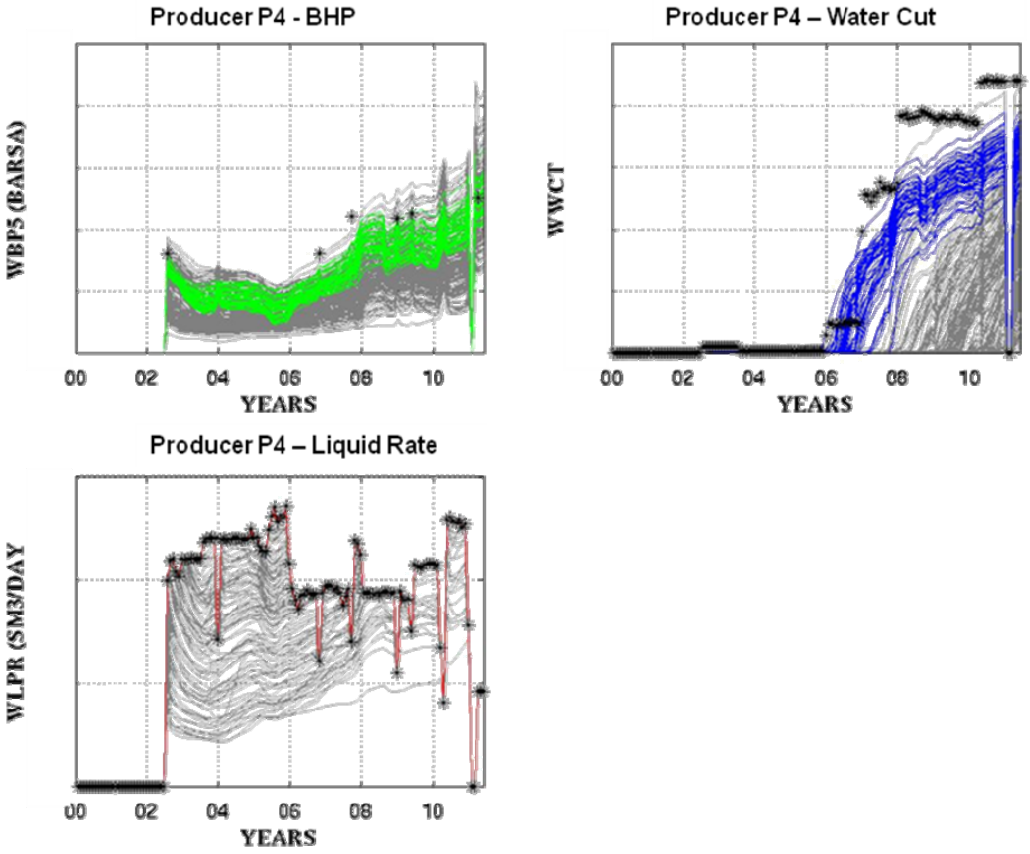

Figure 12 *History match results for Producer P4.*

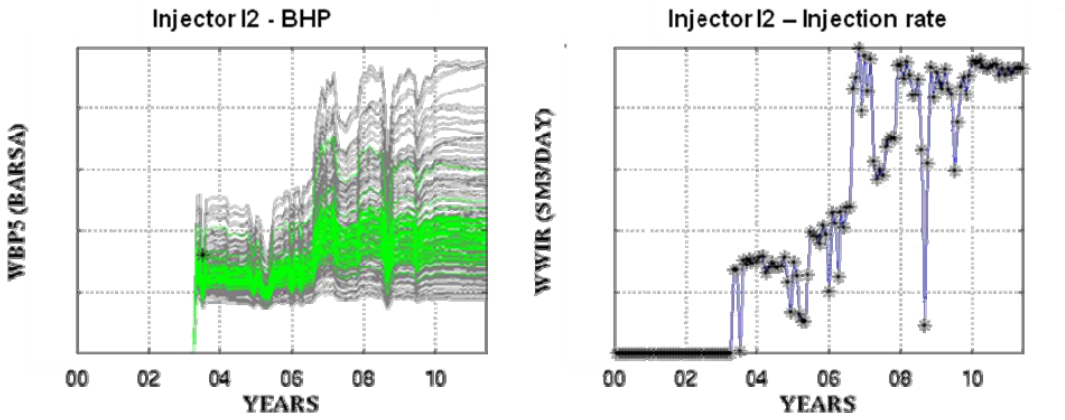

Figure 13 *History match results for Water Injector I2.*

Properties update with EnKF

In order to evaluate the history match quality, a final check on the updated reservoir properties was performed. The initial and final mean of the ensemble for Ln-K and the corresponding standard deviation respectively before and after the EnKF update are reported in *Figure 14*. The final permeability map is in line with the geological interpretation. As expected, there was a general reduction of uncertainty after the EnKF integration. However, the uncertainty range of the final ensemble is well maintained also thanks to the localization strategy. *Figure 15* shows the correlation between porosity and LnK in one of the main layer for the initial (blue) and final (red) ensemble: the correlation is preserved even after the EnKF assimilation. In conclusion, the final petrophysical properties are consistent to the geological framework.

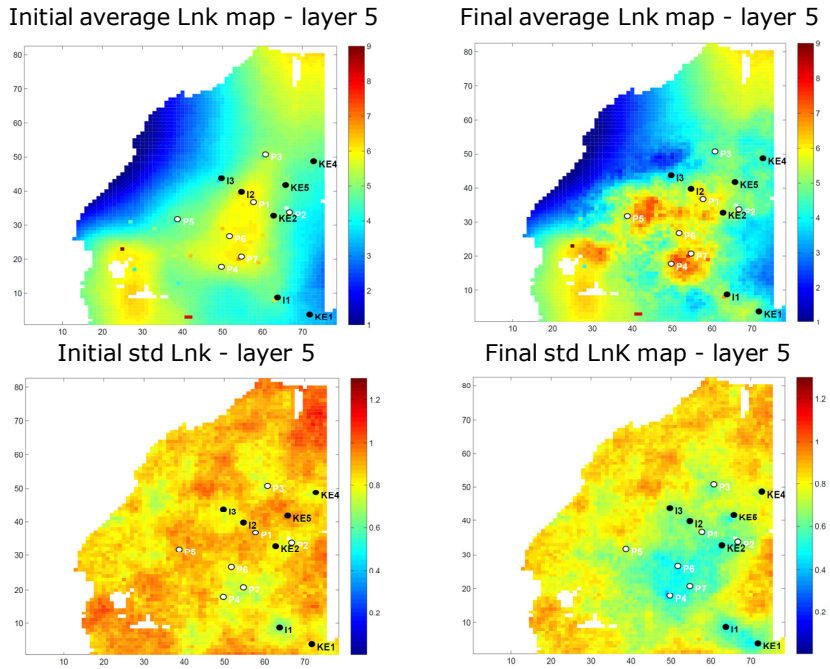

Figure 14 *Initial and final ensemble mean and standard deviation Ln-K map for layer 5.*

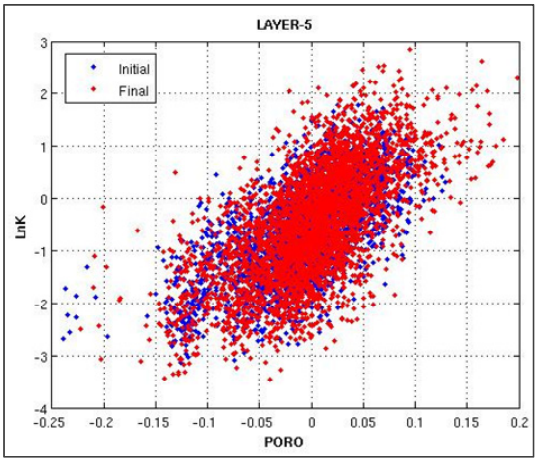

Figure 15 *Porosity-permeability relationship in layer 5 of the initial (blue) and final (red) ensemble.*

The boxplot of the distribution of water relative permeability at the critical oil saturation (Krwr) at the different assimilation steps is reported in *Figure 16*. The EnKF has no influence in the parameter update until the water injection start up (assimilation step 30). From that moment on, the EnKF increases the Krwr values. The final average Krwr value is about 0.45 in line with the expectations for a mixed wettability environment, [22].

Moreover, the EnKF update for the transmissibility of two main faults is represented in *Figure 17* and *Figure 18*. The EnKF gave a clear indication about the sealing capacity of fault 1 (indicated in green in *Figure 8*) and the transmissibility of fault 4 (indicated in black in *Figure 8*) in order to improve the history match quality. The EnKF did not show relevant effects on other faults.

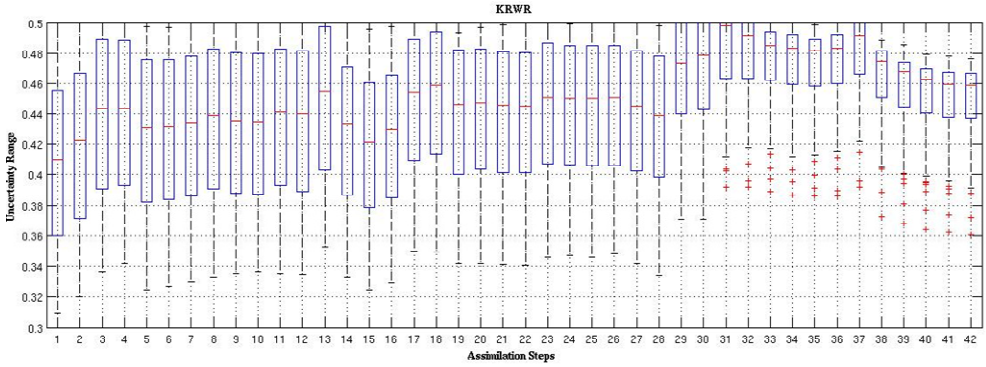

Figure 16 *Box plot of Krwr distribution at each assimilation step.*

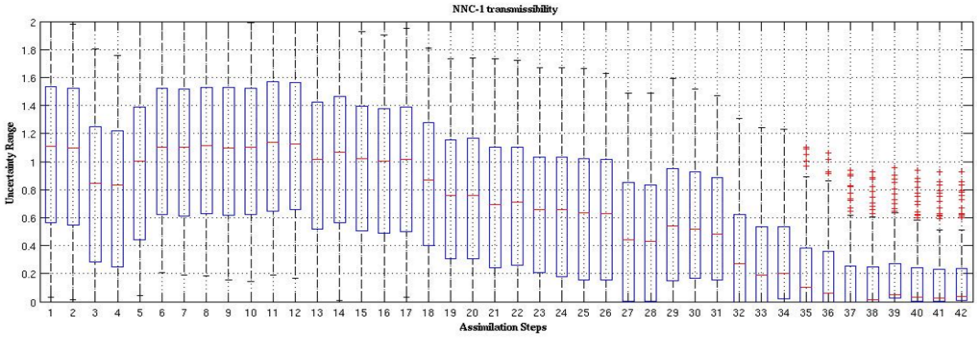

Figure 17 *Box plot of transmissibility distribution for the fault 1 at each assimilation step.*

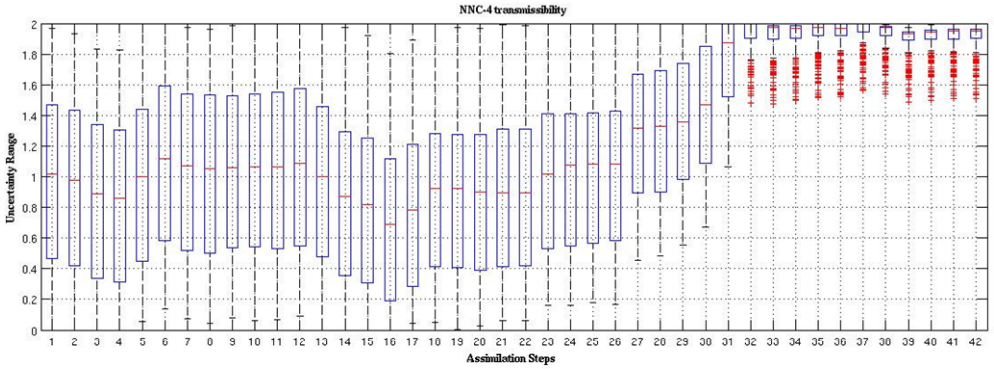

Figure 18 *Box plot of transmissibility distribution for the fault 4 at each assimilation step.*

Optimization of polymer injector location

Moving from history matching to production forecast, a screening analysis was the first step to identify the optimal position of the injection well for a disperse water-polymer injection scheme pilot. In order to take into account the uncertainty coming from different geological models, the screening was performed considering the average oil saturation map of the ensemble at the end of the historical production period.
In literature, successful polymer projects are associated to disperse injection in reservoirs with high oil saturation and low actual recovery, [21], [18], [10], [20], [12]. These conditions could be found in the eastern flank of the pilot area, characterised by low water saturation as demonstrated by the average oil saturation map of the ensemble after history matching, see *Figure 19*.

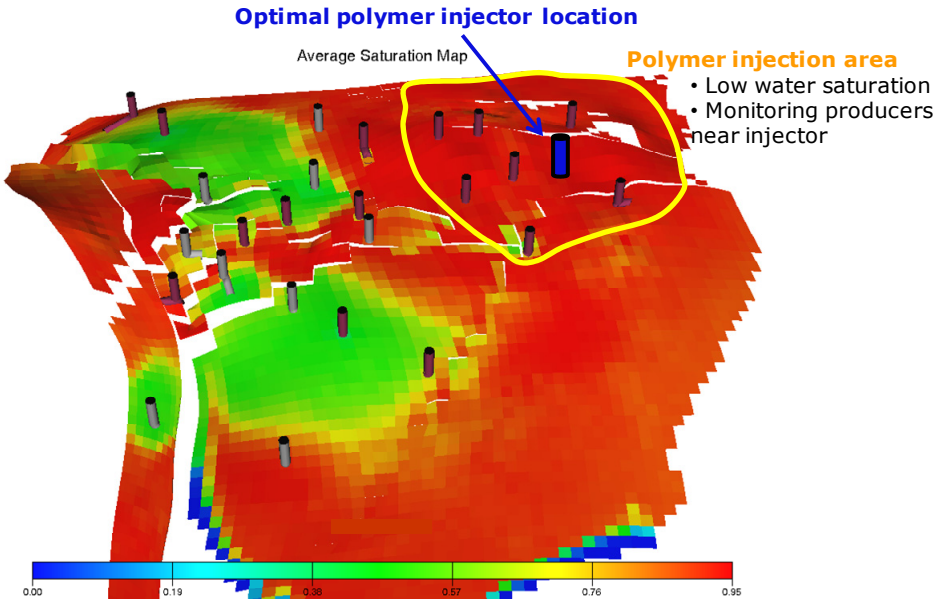

Figure 19 *Polymer injector optimal location determined based on the average oil saturation map of the ensemble.*

The location shown in the picture allows injecting in an unswept area, with the possibility to sweep the drainage area of seven existing wells, producing with water-cut ranging between 0% and 60%.
In the remaining of the paper, these seven surrounding producers will be considered as target wells for the development strategy optimization. Therefore, all the production profiles presented later on are the sum of each single target well profile.

According to the polymer flood model, the reservoir simulator has been tuned according to the results of the laboratories analysis [3].

In addition, the hydraulic communication of the pilot area with other reservoirs calls for a perfect coupling between the EOR and the full field development strategy. The polymer flooding was evaluated over the next 10 years forecast. In this time lapse, according to the full field development strategy, the average pressure of the pilot area is expected to be maintained higher than other reservoirs. This condition is guaranteed by the presence of calibrated dummy water producers.

Ensemble based optimization of polymer development strategy

Once the injector location was selected using a standard polymer strategy, a detailed optimization of the polymer development strategy was performed.
The starting point was the ensemble of sector models constrained to geological and production data obtained with the EnKF, which represents the uncertainty in the field at the state of art. Including all the alternative geological realizations in a manually optimized development plan would have been unfeasible. On the other side, optimizing a single reference model would have created a major risk of underestimating uncertainty. Therefore, an ensemble based optimization technique (EnOpt) was implemented, [6], [7], [7].
EnOpt uses the steepest ascent method to maximise an objective function g by approximating the sensitivity of g with respect to the optimization variables with averages computed on the basis of coupled ensemble of controls (optimization parameters) and geological models. In particular, EnOpt starts with the definition of the base development strategy, the control variables ($x_1, x_2, \ldots, x_{N_c}$) and the objective of the optimization g. Examples of typical controls variables for polymer flooding are injection rates and polymer concentrations. The objective is generally the maximization of the Net Present Value (NPV). Once controls and objective are defined, EnOpt creates the coupled ensemble of controls and geological models. This ensemble is generated by perturbing the control variables $\{\mathbf{x}_j\}_{j=1}^{N_e}$ and then coupling it with the ensemble of matched models $\{\mathbf{y}_j^u\}_{j=1}^{N_e}$ after the EnKF: $\{\mathbf{y}_j^u, \mathbf{x}_j\}_{j=1}^{N_e}$. The objective function is then computed as average among all the models of the coupled ensemble: if NPV is considered, we have $g = \frac{1}{N_e}\sum_{j=1}^{N_e} NPV(\mathbf{y}_j^u, \mathbf{x}_j)$ (this step requires N_e simulation runs). During the iteration loop, the ensemble of controls is continuously updated. In particular, let ℓ, the iteration index, and let $\{\mathbf{y}_j^u, \mathbf{x}_{\ell,j}\}_{j=1}^{N_e}$ the ensemble of controls at iteration ℓ with objective $g(\mathbf{x}_\ell)$, the algorithm follows the following procedure.

- *Compute gradients* – The output from the ensemble of models is used to approximate gradients to the control variables:

$$C_g = \frac{1}{N_e - 1}\sum_{j=1}^{N_e}(\mathbf{x}_{\ell,j} - \overline{\mathbf{x}_\ell})(g(\mathbf{y}_j^u, \mathbf{x}_{\ell,j}) - \overline{g(\mathbf{y}^u, \mathbf{x}_\ell)}),$$

  with $\overline{\mathbf{x}_\ell} = \frac{1}{N_e}\sum_{j=1}^{N_e}\mathbf{x}_{\ell,j}$ and $\overline{g(\mathbf{y}^u, \mathbf{x}_\ell)} = \frac{1}{N_e}\sum_{j=1}^{N_e} g(\mathbf{y}_j^u, \mathbf{x}_{\ell,j})$.

- *Update controls* - Using gradient, the ensemble of controls is updated with $\mathbf{x}_{\ell+1} = \frac{1}{\alpha_l} C_g + \mathbf{x}_\ell$ where α_ℓ is a tuning parameter that determines the step size in the steepest ascent direction.

- *Run flow simulation and compute objective function* – Flow simulation is run on each member of the updated ensemble and the objective function $g(\mathbf{x}_{\ell+1})$ are computed.

- *Check objective function* - If $g(\mathbf{x}_{\ell+1}) > g(\mathbf{x}_{\ell})$, overwrite $\mathbf{x}_{\ell+1}$ by $\mathbf{x}_{\ell}$ and let $\ell = \ell + 1$, otherwise keep $\mathbf{x}_{\ell}$, increase α_{ℓ} and continue the loop.

The loop continues till some stopping criteria on percentage increment of the objective function are met.

In the above procedure, the update is addressed only to the ensemble of controls while the ensemble of geological models $\{\mathbf{y}_j^u\}_{j=1}^{N_e}$ is fixed. However, coupling the ensemble of controls with the ensemble of geological models allows performing a "robust" optimization on the expected value over all the realizations taking into account the remaining geological uncertainty of the matched models. EnOpt can be also integrated in a more general closed-loop framework of data assimilation and production optimization, [6], [7], [7].

Base case development strategy and EnOpt implementation in the sector model

The forecast scenario was evaluated over a period of 10 years. Generally the base development strategy for a polymer injection consists of an initial short water injection pre-flush followed by multiple polymer slugs at different concentrations. A final water flooding can be used to push the polymer slugs towards the surrounding producers improving the mobility ratio and saving on the polymer cost.
In this paper, after 3 months of water pre-flush, three different polymer slugs were optimized followed by a final water injection until the end of the forecast simulation.
The polymer development strategy was optimized choosing as control variables the polymer concentrations and the time length of each of the three slugs:

$$\mathbf{x} = (conc_1,\ tstep_1, conc_2, tstep_2, conc_3,\ tstep_3).$$

The polymer injector is under BHP control.
The controls variables were perturbed within specified ranges to create the control ensemble with 100 members.
The objective function was set to maximize the average NPV over the entire ensemble at the end of the forecast period:

$$NPV = \sum_{i=i}^{N_t} \frac{(Q_{o_i} * p_o - Q_{w_i} * p_w - Q_{p_i} * p_p) - CAPEX}{(1 + r_T)^{t_i/T}}$$

where i is the time step index, N_t is the total number of time steps, r_T is the discount rate for the reference time interval T and t_i is the cumulative time since the start of production. p_o, p_w and p_p are the price of oil, the cost of water disposal and the cost of the polymer, respectively. Q_o and Q_w are the total oil and water production over time step Δt of the wells close to the polymer injector and Q_p is the total polymer injected over Δt.

In our specific case the reference values are:

- Oil price = 90 $/barrel;
- Produced water cost = 1 $/barrel;
- Polymer cost = 4.25 $/Kg;
- CAPital EXpenditure (CAPEX) (including the drilling of the new injector and the additional surface facilities for the polymer treatment) = 9.6*10^6 $;
- Discount rate = 10%.

In our case, the range of variability of the final cumulative oil rising from the 100 geological models was very large and strongly dependent on the petrophysical properties. Therefore, coupling the ensemble of controls with all the geological realizations made the gradient computation difficult to be correctly executed. In order to avoid this problem, only 5 realizations $\{\mathbf{y}_r^u\}_{r=1,..,5}$ were selected to be coupled with the ensemble of 100 engineering controls. In particular, it is worth to indicate with

$\{\mathbf{y}_{r_j}^u, x_{\ell,j}\}_{j=1}^{N_e}$ the coupled ensemble where r_j varies repetitive from 1 to 5 (so each realization is coupled with 20 perturbed controls). The 5 realizations were selected in order to represent the range of variability of oil in place over all the different geological models. During the EnOpt loop, after running the flow simulation for the 100 reservoir models, the gradient was computed in two steps:

- First, the ensemble was divided in 5 (based on the realization number) and 5 separate gradients C_{g_r} were computed with the EnOpt formula:

$$C_{g_r} = \frac{1}{N_e/5} \sum_{j:r_j=r} (\mathbf{x}_{\ell,j} - \overline{\mathbf{x}_\ell})(g(\mathbf{y}_{r_j}^u, \mathbf{x}_{\ell,j}) - \overline{g(\mathbf{y}^u, \mathbf{x}_\ell)})$$

  with $\overline{\mathbf{x}_\ell} = \frac{1}{N_e/5} \sum_{j:r_j=r} \mathbf{x}_{\ell,j}$ and $\overline{g(\mathbf{y}^u, \mathbf{x}_\ell)} = \frac{1}{N_e/5} \sum_{j:r_j=r} g(\mathbf{y}_{r_j}^u, \mathbf{x}_{\ell,j})$.

- Then, the final gradient was calculated as sum of the partial gradients $C_g = \sum_{r=1}^{5} C_{g_r}$

Using this procedure, the difficulties in the gradient computation were overcome and the different scale of variability of the objective function were correctly captured. Moreover, the final gradient has demonstrated to be able to move the whole ensemble towards optimal values.

Optimization results in the sector model

Figure 20 shows the trend of the average NPV after 30 optimization iterations. As it can be observed, the trend is monotonically increasing with a steeper slope at the beginning while at the end the optimization starts to converge.
In order to validate the results, the optimized controls were applied over the 100 reservoir models and the results compared to the do-nothing scenario and to an equivalent water injection scenario. Finally, statistics concerning P10, P50, and P90 profiles were analyzed.
Figure 21 shows the P50 profile for the oil rate of the target wells regarding the do-nothing, the water injection and the optimized polymer scenarios. The optimization strategy is also illustrated: after an initial short water pre-flush, a first polymer slug with relatively low viscosity (3cP) is injected followed by a higher viscosity slug (6.5cP). In the end, the polymer is pushed towards the surrounding producers by water flooding. As expected, the polymer injection gives a benefit in terms of P50 oil rate with respect to the other scenarios. In terms of cumulative oil production, the water injection is supposed to give an average incremental recovery of 10% compared to the do-nothing case. However, the optimized polymer injection is expected to increment the average recovery by 16%, see *Figure 22*.

Moreover, the polymer strategy reduces the produced water by 11%, *Figure 23*. The results are summarized in *Figure 24*.

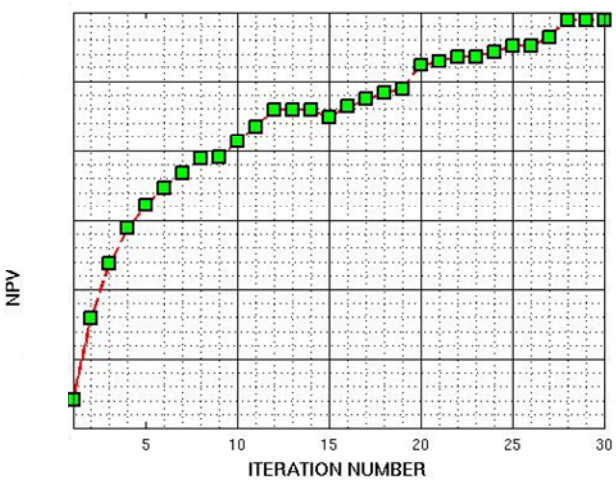

Figure 20 *EnOpt optimization: average NPV versus iterations.*

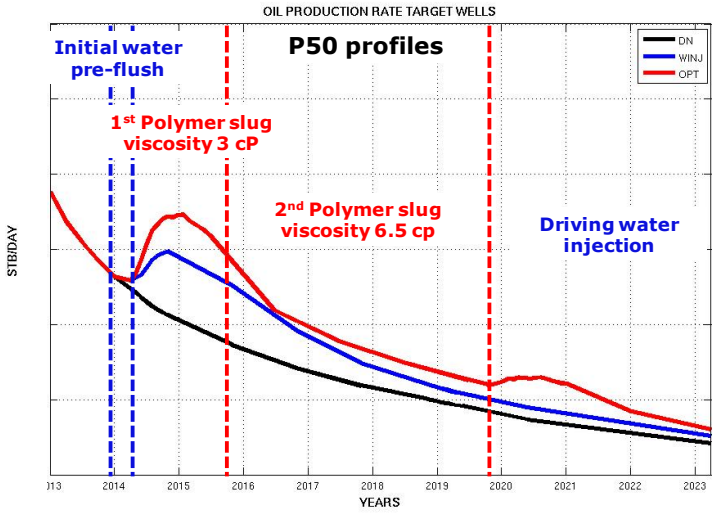

Figure 21 *Oil production rate of target wells: p50 of do-nothing (black), water injection (blue), optimized (red) scenarios.*

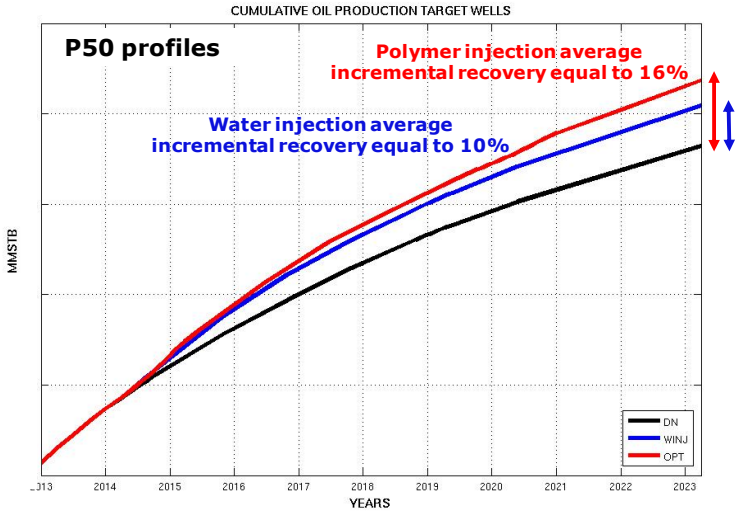

Figure 22 *Cumulative oil production rate of target wells: p50 of do-nothing (black), water injection (blue), optimized (red) scenarios.*

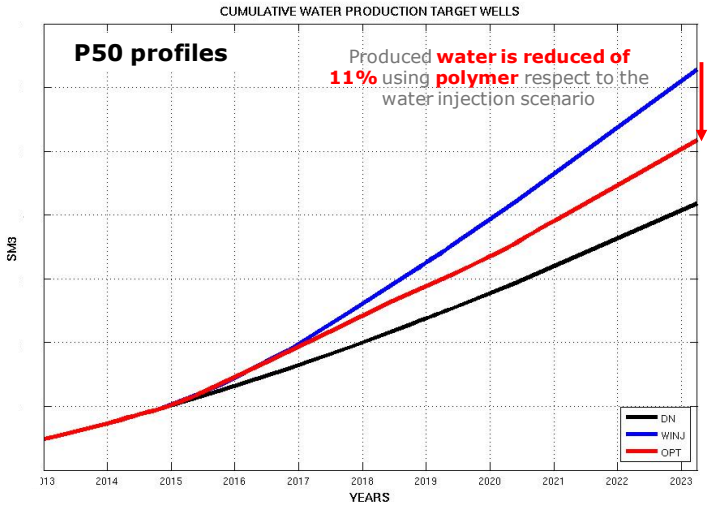

Figure 23 *Cumulative water production rate of target wells: p50 of do-nothing (black), water injection (blue), optimized (red) scenarios.*

Development scenario	Additional Oil Production at 2023 (P50)	Additional technical NPV at 2023 (P50)
	%	%
Actual	-	-
Water Inj.	+ 10 %	+ 3 %
Polymer Inj.	+ 16 %	+ 8 %

Figure 24 *EnOpt optimization: results summary compared to the do-nothing scenario.*

Conclusions

Multiple high resolution sector models were built integrating all the available data and taking into account geological and dynamical uncertainties. First, the ensemble of models were history matched using the Ensemble Kalman filter technique. Secondly, the matched ensemble were used to optimize both the polymer injector location and the development strategy. The following conclusions can be drawn.

- Production data for wells in commingle were retrieved using the full field model and the hydraulic communication with other reservoirs was managed through the introduction of dummy wells.
- Multiple geological and dynamic models were realized honouring all the available data (including the new RCAL and SCAL) to represent the uncertainty of the reservoir.
- Using the EnKF, a good quality history match for the 100 alternative reservoir models was achieved. The geological coherence was maintained without any manual modifications. Therefore, the ensemble of matched models represents a valid starting point to evaluate the range in forecast production.
- A robust optimization of the polymer development strategy was performed using the EnOpt approach.
- The polymer flooding confirmed to be a cost-effective EOR technique for the field. The optimized development strategy foresees to obtain an improvement of the average cumulative oil production of 16% in ten year time. Moreover, an increment of 8% is expected in terms of average NPV.
- A closed loop workflow was applied to manage multiple models both for history matching and production forecast optimization.

Acknowledgements

We would like to thank eni exploration & production division and Ieoc Production B.V. for the permission to publish this paper. We also would like to thank Yan Chen from IRIS for his helpful suggestions and technical support.

References

[1] Aanonsen, S.I., Nævdal, G., Oliver, D.S. and Reynolds, A.C. [2009] The ensemble Kalman filter in reservoir engineering - a review. *SPE J.*, **14**(3), 393-412.
[2] Anderson, J.L. [2007] Exploring the need for localization in ensemble data assimilation using a hierarchical ensemble filter. *Physica*, D 230, 99-111.
[3] Bianco, A., Cominelli, A., Dovera, L., Nævdal, G. and Valles, B. [2007] History matching and production forecast uncertainty by means of the ensemble Kalman filter: a real field application. *SPE 107161, SPE Europec/EAGE Annual Conference*, London, United Kingdom, 11-14 June, 2007.
[4] Braccalenti, E., Albonico, P., Romero-Zeron, L., Parassiliti Parracello, V., Masserano, F. and Del Gaudio, L. [2013] Polymer flooding – designing of a pilot test for an unusually high salinity and hardness reservoir. *EAGE IOR Symposium*, Saint Petersburg, Russia, 16-18 April 2013.
[5] Burgers, G., van Leeuwen, P.J. and Evensen, G. Analysis scheme in the ensemble Kalman filter. *Mon. Weather Rev.*, **126**, 1719-1724.
[6] Chen, Y., Oliver, D. and Dongxiao, Z. [2009] Efficient ensemble-based closed-loop production optimization. *SPE J.*, **14**(4), 634-645.
[7] Chen, Y., Oliver, D. [2012] Localization of ensemble-based control-setting updates for production optimization. *SPE J.*, **17**(1), 122-136.
[8] Chen, Y. and Oliver, D. [2009] Ensemble-based closed-loop optimization applied to Brugge field. *SPE 118926, SPE Reservoir Simulation Symposium*, The Woodlands, Texas, USA 2-4 February 2009.

[9] Cominelli A., Dovera L., Vimercati S. and Nævdal G. [2009] Benchmark study of ensemble Kalman filter methodology: history matching and uncertainty quantification for a deep water oil reservoir. *International Petroleum Technical Conference 2009*, IPTC 13748, Doha, Qatar.

[10] Demin, W., Jiecheng, C., Junzheng, W. and Gang, W. [] Experience learned after production more than 300 million barrels of oil by polymer flooding in Daquing oil field. *SPE 77693, Annual Technical Conference and Exhibition*, San Antonio, USA 29 September – 2nd October 2002.

[11] Deutsch, C.V. and Journel, A.G. [1998] *Geostatistical software library and user's guide*. Oxford University Press.

[12] Du, Y. and Guan L. [2004] Field-scale polymer flooding: lessons learnt and experience gained during past 40 years. *SPE 91787, International Petroleum Conference*, Puebla, Mexico, 8-9 November 2004.

[13] Evensen, G. [1994] Sequential data assimilation with a nonlinear quasi-geostrophic model using Monte Carlo methods to forecast error statistics. *J. Geophys. Res*., **99**, 10143-10162.

[14] Furrer, R. and Bengtsson, T. [2007] Estimation of high-dimensional prior and posterior covariance matrices in Kalman filter variants. *J. Multivar. Anal*., **98**, 227-255.

[15] Gaspari, G. and Cohn, S.E. [1999] Construction of correlation functions in two and three dimensions. *Q.J.R. Meteorol. Soc*., **125**(554), 723-757.

[16] Jansen, J.D., Douma, S.D., Brouwer, D.R., Van den Hof, P.M.J., Bosgra, O.H. and Heemink, A.W. [2009] Cloosed-loop reservoir management. *SPE 119098, SPE Reservoir Simulation Symposium*, The Woodlands, Texas, USA 2-4 February 2009.

[17] Mandel, J., Cobb, L. and Beezley, J.D. [2011] *On convergence of the ensemble Kalman filter*. arXiv:0901.2951v2.

[18] Morel, D., Vert, M., Jouenne, S., Nahas, E. [2008] Polymer injection in deep offshore field : the Dalia Angola case. *SPE 116672, Annual Technical Conference and Exhibition*, Denver, USA, 21-24 September 2008.

[19] Nævdal, G., Johnsen, L.M., Aanonsen, S.I. and Vefring, E.H. [2005] *Reservoir monitoring and continuous model updating using ensemble Kalman filter*. *SPE J*., **10**(1), 66-74.

[20] Panday, A., Beliveau, D., Corbishley, D.W., Kumar, M.S. [2008] Design of an ASP pilot for the Mangala field: laboratory evaluations and simulation studies. *SPE 113131, Indian Oil and Gas Technical Conference and Exhibition*, Mumbai, India, 4-6 March 2008.

[21] Shehata, A.M., Ghats, A., Kamel, M., Aly, A., Hassan, A. [2012] Overview of polymer floding (EOR) in north Africa fields – elements of designing a new polymer/surfactant flood offshore (case study). *SPE 151952, North Africa Technical Conference and Exhibition*, Cairo, Egypt 20-22 February 2012.

[22] Stiles, J. *Special Core Analysis*. Hot Engineering GmBH, Leoben, Austria.